Energy Conversion and Management 80 (2014) 71–77

Contents lists available at ScienceDirect

Energy Conversion and Management

journal homepage: www.elsevier.com/locate/enconman

Theoretical and experimental study of sheet and tubes hybrid PVT collector

K. Touafek *, A. Khelifa, M. Adouane

Unité de Recherche Appliquée en Energies Renouvelables, URAER, Centre de Développement des Energies Renouvelables, CDER, 47133 Ghardaïa, Algeria

ARTICLE INFO

Article history:
Received 22 September 2013
Accepted 13 January 2014
Available online 6 February 2014

Keywords:
Hybrid
Photovoltaic
Thermal
Modeling
Experimental
Tube
Galvanized steel
Temperature

ABSTRACT

Electrical performance of the hybrid photovoltaic thermal (PVT) collector may improved at increased intensity of solar radiation if the system is set to extract heat from solar cells, which is cooled at the same time. The objective of this work is to study theoretically and experimentally a new configuration of the PVT system which extracts heat from the photovoltaic module. This configuration is tube and sheet integrated into a prototype and tested at the unit of applied research in renewable energy Ghardaïa in the south of Algeria. The advantages of this hybrid collector are better heat absorption and lower production cost compared to other configurations of hybrids collectors.

1. Introduction

The solar hybrid collectors are the fundamental elements in the transformation of solar energy into thermal and electrical energy; this allows an increase in the overall total conversion efficiency of solar energy received. Research on solar began in the 1970s and has been intensified in the 1980s. In 2005, Zondag [1] provides a state of the art on the solar PVT hybrid based on the report of the European project PV-Catapult [2]. Among the first studies reviewed by Zondag [1], some of them focus on the evolution of the geometry and other components of modeling methods. Thus, Wolf [3] in 1976 performs the analysis of a solar thermal collector coupled to a heat storage system with PV modules based on silicon. Subsequently, the study by Kern and Russel in 1978 gives the basics of using solar water or air as a coolant. In 1982, Hendrie [4] developed a theoretical model of PVT hybrid collector based on correlations related to solar standards. In 1981, Raghuraman [5] presents numerical methods for predicting the performance of flat solar PVT water or air. Later, in 1985, Cox and Raghuraman [6] developed simulation software to study the performance of air hybrid PVT and focus on the influence of the optical properties of the glazing on the thermal performance and electrical components of solar. In 1986, Lalovic et al. [7] propose a new type of transparent amorphous a-Si cells as a cost effective solution for the construction of PV modules. Various experimental and theoretical studies have been carried out then, for the development of PVT hybrid collectors [8]. In 1997, Fujisawa and Tani [9] have designed and built solar hybrid PVT water on a university campus in Tokyo, Japan. In 2003, solar PVT hybrid water is investigated under dynamic conditions by Chow [10] which achieves an appropriate model for transient thermal simulations. It relies on the work of Bergen and Lovvik [11] that present in 1995. Chow et al. [12] presented the modeling and a comparison of the performance of solar PVT hybrid water, a solar PV and solar water. Two prototype solar hybrid collectors have been built, the first having been modeled in 2006 [13]. Other PVT systems have been investigated and discussed by many researchers for the last decade in the literature [14–21].

The design idea of the hybrid collector with galvanized steel sheet and tube as absorber came after it was noticed in previous studies and designs [22] which note that the simple galvanized steel configuration absorber is not very interesting because the raison of low heat exchange in the top layer of the absorber. The sheet and tube configuration which is adapted in the design of plan thermal collectors is used. On top of that, we used galvanized steel for its low cost [23]. In this paper, a model of this hybrid collector is performed by determining the temperatures levels on these layers and the influence of some parameters on electrical and thermal performance is studied. A comparison with other existing configurations is made. An experimental study was initiated to validate the theoretical results.

* Corresponding author. Tel.: +213 29870150.
E-mail address: khaledtouafek@yahoo.fr (K. Touafek).

0196-8904/$ - see front matter © 2014 Elsevier Ltd. All rights reserved.
http://dx.doi.org/10.1016/j.enconman.2014.01.021

Nomenclature

A	area
C_i	specific heat of node i
C	specific heat
cel	solar cell
D	inside diameter of the tube
F	fin efficiency
f	fluid
FR	factor extraction of heat from the collector
G	global irradiance
h_f	exchange coefficient by convection in tube
$h_{c\text{-}a}$	exchange coefficient by convection with the ambient
h_{cond}	exchange coefficient by conduction
h_{conv}	exchange coefficient by convection
h_{rad}	exchange coefficient by radiation
iso	insolation
L	length of tube
M_i	mass of node i
M	mass
$\dot{m}$	mass flow rate
N	number of glass
n	number of tubes
PVT	photovoltaic thermal
p	plate
Q_{th}	thermal energy
Q_{ele}	electric energy
t	tube
Ted	Tedlar
T	temperature
T_{pm}	average temperature of the absorber
T_a	ambient temperature
T_s	output temperature of the fluid
T_e	input temperature of the fluid
T_{ciel}	temperature of Sky
T_{cel}	temperature of cell
T_{ted}	temperature of Tedlar
T_p	temperature of plat absorber
T_t	temperature of tube
T_f	temperature of fluid
T_{av1} PVT	temperature of the upper part of glass
T_{av2} PVT	temperature of the lower part of glass
T_{isoint}	internal temperature of the insulation
T_{isoext}	external temperature of the insulation
Q	heat flux
$U_{p\text{-}a}$	loss ratio
W	distance between two tubes
λ	thermal conductivity
ε	emissivity
$\tau\alpha$	absorptivity–transmittivity factor
v	glass
V	speed
τ	transmissivity
μ	viscosity of water
σ	Stefan–Boltzmann constant
α_{cel}	absorptivity coefficient of the solar cell
α	ideality factor of the photovoltaic cell
δ	thickness
η	efficiency

2. Modeling of hybrid PVT collector

PVT hybrid collector (Fig. 1) consists of the PV module with a thermal absorber made of sheet and tube housed in a metal enclosure which includes thermal insulation.

Fig. 2 shows the equivalent circuit diagram of the hybrid collector containing the thermal absorber.

Fig. 2 shows the energy balance used for the various layers constituting the hybrid collector, where Q_{sun} is the energy emitted by the sun on the glass of the hybrid collector, Q_{rad} the energy emitted by the sky by radiation on the glass of the hybrid collector, Q_{conv} the energy emitted by the ambient air by convection on the glass of the hybrid collector, $Q_{cel\text{-}v}$ the thermal output by conduction from the glass to the solar cells, $Q_{cel\text{-}plat}$ the thermal output by conduction from the lower layer of the solar cells to the absorber plat, Q_{ele} the electrical output by the solar cell Q_{th} the thermal output from the layer of the absorber plat to the coolant, Q_{ins} the thermal output by the conduction from the lower layer of the absorber plat to the internal layer of the insulation. Seven layers exist in all: three layers constituting the photovoltaic module (tempered glass, silicon cells, Tedlar), layer of the upper part of the absorber, the coolant, the lower layer of the absorber, and finally, the layer of the insulation.

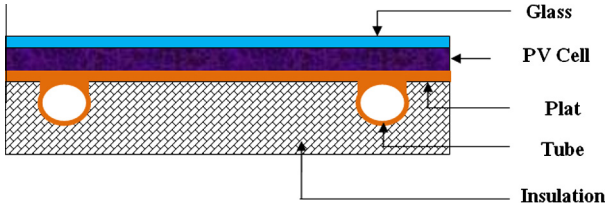

Fig. 1. Model of PVT hybrid collector.

Change in internal energy = Energy received–Energy lost

$$M_i C_i \frac{dT_i}{dt} = \sum_r Q_i - \sum_s Q_i \quad (1)$$

r: received energy
s: lost energy

The thermal energy supplied by solar radiation is given as follows [16]:

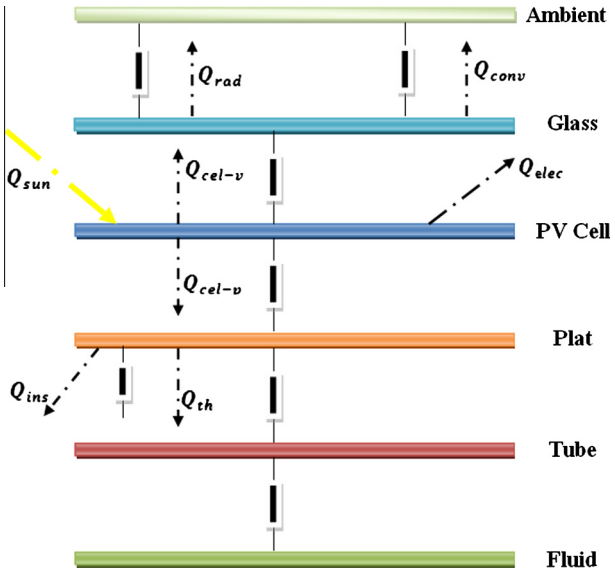

Fig. 2. Equivalent circuit diagram of the hybrid collector.

$$Q_{sun} = A_{glass} G \tau_{glass} \alpha_{cel} \quad (2)$$

$$Q_{radv\text{-}ciel} = \sigma \varepsilon_v A_{glass} (T_v^4 - T_{ciel}^4) \quad (3)$$

$$T_{ciel} = 0.0552 (T_a)^{1.5} \quad (4)$$

$$Q_{convv\text{-}a} = h_{c-a} A_{glass} (T_v - T_a) \quad (5)$$

$h_{c\text{-}a}$: convective transfer coefficient which depends on the wind speed (W/m^2 K) is given by the following expression [22]:
$Q_{radv\text{-}ciel}$: heat transfer emitted by the sky by radiation on the glass;
$Q_{convv\text{-}a}$: heat transfer emitted by the ambient air by convection on the glass;
Q_{condv}: conductive heat transfer from the top to the bottom of glass.

$$h_{c\text{-}a} = 2.8 + 3.0 V_{wind} \quad (6)$$

On the outside of the glass:

$$M_v C_v \frac{dT_{vext}}{dt} = Q_{sun} - Q_{radv\text{-}ciel} - Q_{convv\text{-}a} - Q_{condv} \quad (7)$$

On inside of the glass:

$$M_v C_v \frac{dT_{vint}}{dt} = Q_{sun} + Q_{condv} - Q_{condv\text{-}cel} \quad (8)$$

$$M_v C_v \frac{dT_{vint}}{dt} = A_{glass} G \tau_{verre} \alpha_{cel} + h_{condv} A_{glass} (T_{vext} - T_{vint}) - h_{condv\text{-}cel} A_{glass} (T_{vint} - T_{cel}) \quad (9)$$

$$h_{condv} = \frac{\lambda_v}{\delta_v}$$

λ_v: thermal conductivity of glass;
δ_v: thickness of glass;
$Q_{condv\text{-}cel}$: conductive heat transfer from the glass to the cell;
$h_{condcel}$: exchange coefficient by conduction from the bottom of glass to the cell;
$h_{condcel\text{-}ted}$: exchange coefficient by conduction from the cell to the Tedlar.

For the solar cell

$$M_{cel} C_{cel} \frac{dT_{cel}}{dt} = Q_{condcel} - Q_{condcel\_ted} - Q_{ele} \quad (10)$$

$$M_{cel} C_{cel} \frac{dT_{cel}}{dt} = h_{condcel} A_{cel} (T_{cel} - T_{vint}) - h_{condcel\text{-}ted} A_{cel} (T_{cel} - T_{ted}) - Q_{ele}$$

$$h_{condcel} = \frac{\lambda_{cel}}{\delta_{cel}}, h_{condcel\text{-}ted} = \frac{1}{\frac{\delta_{cel}}{\lambda_{cel}} + \frac{\delta_{ted}}{\lambda_{ted}}}$$

$$Q_{ele} = \frac{Q_{sun}}{\alpha_{cel}} \eta_{ref} \exp(\beta (T_{cel} - T_{ref})) \quad (11)$$

λ_{cel}: thermal conductivity of cell; δ_{cel}: thickness of cell;
η_{ref}: reference efficiency measured for a reference temperature taken as 25 °C;
β: the temperature coefficient (about 0004 for a silicon solar cell) [22].
T_{ref}: reference temperature of cell;
$Q_{condcel}$: conductive heat transfer from the bottom of glass to the cell;
$Q_{condted}$: conductive heat transfer from the cell to the Tedlar.

For Tedlar:

$$M_{ted} C_{ted} \frac{dT_{ted}}{dt} = Q_{condted} - Q_{condted\text{-}p} \quad (12)$$

$$M_{ted} C_{ted} \frac{dT_{ted}}{dt} = h_{condted} A_{ted} (T_{ted} - T_{cel}) - h_{condted\text{-}p} A_{ted} (T_{ted} - T_p) \quad (13)$$

$$h_{condted} = \frac{\lambda_{ted}}{\delta_{ted}}, h_{condted\text{-}p} = \frac{1}{\frac{\delta_{ted}}{\lambda_{ted}} + \frac{\delta_p}{\lambda_p}}$$

λ_{ted}: thermal conductivity of Tedlar;
δ_{ted}: thickness of Tedlar;
$Q_{condted\text{-}p}$: conductive heat transfer from the Tedlar to the absorber plat.

At the absorber plate.

Fig. 3 shows that each element of the tube receives an input of energy from each side. Considering the significant temperature gradient in the direction of fluid flow.

So the total transfer rate per unit length in the direction of flow of the coolant is expressed by:

$$q_u = [(W - D_{ext})F + D_{ext}][S - U_{p\text{-}a}(T_{base} - T_a)] \quad (14)$$

The absorber must transfer its heat to the fluid in the tube; the transfer rate can be expressed as:

$$q_u = \frac{T_{base} - T}{\frac{1}{h_f \pi D_{int}} + \frac{1}{C_b}} \quad (15)$$

C_b: The thermal conductance of the solder.

In general, the conduction of the weld is very large, and can be therefore neglected $\frac{1}{C_b} \approx 0$.

By replacing the expression of T_{base} from Eqs. (15) into (14):

$$q_u = WF'[S - U_{p\text{-}a}(T_f - T_a)] \quad (16)$$

F' efficiency that can be calculated as follows:

$$F' = \frac{\frac{1}{U_{p\text{-}a}}}{\frac{1}{W(U_{p\text{-}a}(D_{ext} + (W - D_{ext})F))} + \frac{1}{C_b} + \frac{1}{\pi D_{int} h_{convp\text{-}f}}} \quad (17)$$

According to the conservation energy law:

$$\left[\frac{\dot{m}}{n}\right] C_f T_f|_y - \left[\frac{\dot{m}}{n}\right] C_f T_f|_{y+\Delta y} + \Delta y q_u = 0 \quad (18)$$

$\dot{m}$ is the mass flow of the coolant and n the number of tubes for Δ_y tends to 0, so by replacing the Eqs. (16) into (18), the following differential equation is obtained:

$$\dot{m} C_f \frac{dT_f}{dt} - nWF'[S - U_{p\text{-}a}(T_f - T_a)] = 0 \quad (19)$$

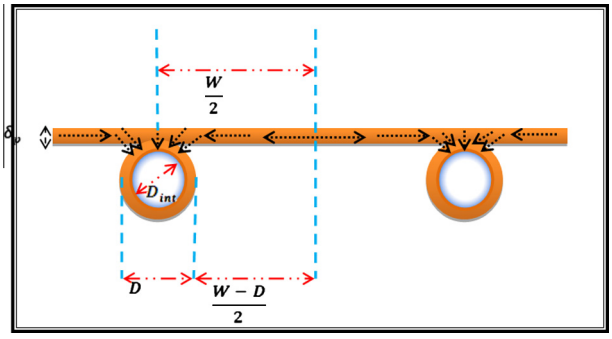

Fig. 3. Energy balance at the absorber plate.

The useful heat can be calculated as follows [24]:

$$Q_{util} = A_{cap}F_R((\tau\alpha)_{PV}G - U_{p\text{-}a}(T_e - T_a)) \quad (20)$$

For the insulation layer.

For the inner layer of insulation, the heat equation is as follows:

$$M_{iso}C_{iso}\frac{dT_{isoint}}{dt} = Q_{condp\text{-}iso} + Q_{condiso\text{-}tube} - Q_{condiso} \quad (21)$$

$$M_{iso}C_{iso}\frac{dT_{isoint}}{dt} = h_{condp\text{-}iso}A_{p\text{-}iso}(T_{isoint} - T_p) + h_{condtube\text{-}iso}A_{iso\text{-}tube}(T_{isoint} - T_t) - h_{condiso}A_{iso}(T_{isoint} - T_{isoext})$$

$h_{condted}$: exchange coefficient by conduction with tedlar and cell;
$h_{condted\text{-}p}$: exchange coefficient by conduction with tedlar and the absorber plat.

$$h_{condiso} = \frac{\lambda_{iso}}{\delta_{iso}}$$

λ_{iso}: Thermal conductivity of Tedlar;
δ_{iso}: thickness of Tedlar.

For the external layer of insulation, the heat equation is as follows:

$$M_{iso}C_{iso}\frac{dT_{isoext}}{dt} = Q_{condiso} + Q_{conviso\text{-}a}$$

$$Q_{condiso} = h_{condiso}A_{iso}(T_{isoext} - T_{isoint})$$

$$Q_{conviso\text{-}a} = h_{conviso\text{-}a}A_{iso}(T_{isoext} - T_a)$$

$$M_{iso}C_{iso}\frac{dT_{isoext}}{dt} = h_{condiso}A_{iso}(T_{isoext} - T_{isoint}) - h_{conviso\text{-}a}A_{iso}(T_{isoext} - T_a)$$

$Q_{condp\text{-}iso}$: conductive heat transfer from the absorber plat to the inner of insolation;
$Q_{condiso\text{-}tube}$: conductive heat transfer from the tube to the inner of insolation;
$Q_{conviso\text{-}a}$: conductive heat transfer from the tube external of insolation to the ambient;
Q_{util}: the useful heat;
n: number of tube;
$A_{p\text{-}iso}$: the surface of contact between the absorber plat and insolation;
$A_{iso\text{-}tube}$: the surface of contact between the tube and insolation;
$h_{condp\text{-}iso}$: exchange coefficient by conduction with absorber plat and the inner layer of insulation;
$h_{condtube\text{-}iso}$: Exchange coefficient by conduction with tube and the inner layer of insulation;
$h_{condiso}$: Exchange coefficient by conduction with the inner the external of insolation.

3. Results and discussions

The resolution of the system is performed by the method of Runge–Kutta (RK4). It is a method of numerical analysis to approximate solution of differential equation.

3.1. Temperature variation

The temperature of an inlet fluid (water) given the change in temperature at each layer that constitutes the hybrid photovoltaic thermal solar collector is determined. Observation of Fig. 4 we can note that the curves of the temporal variation of the temperature in each component of the collector are the same. Moreover, it is easy to see that the highest temperatures are that of the glass, the PV cell, the absorber plate and the inner insulation while the lowest is that of the outer insulation.

Rising temperatures inside and outside of the glass is due to absorption of the incoming solar radiation by the glass and the heat transferred from the surface of the photovoltaic cell by radiation. The temperature of the inner surface is slightly higher than the outside; this is explained by the large amount of flow received

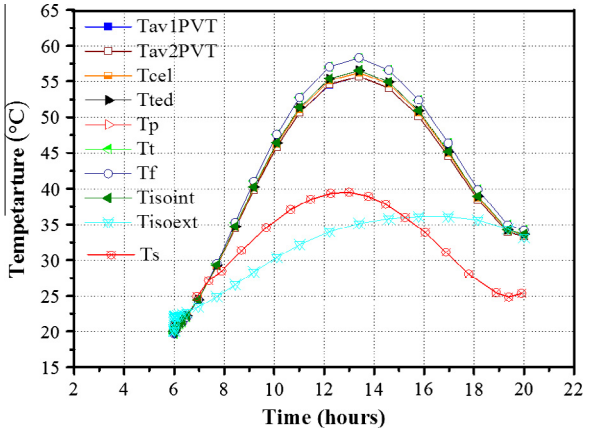

Fig. 4. Temperature variation of PVT layers.

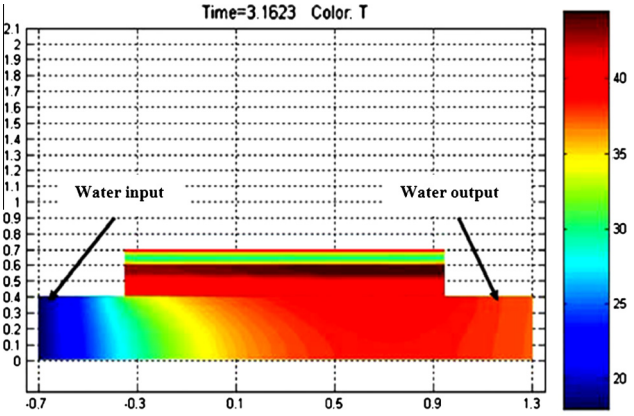

Fig. 5. Temperature distribution in the serpentine hybrid collector.

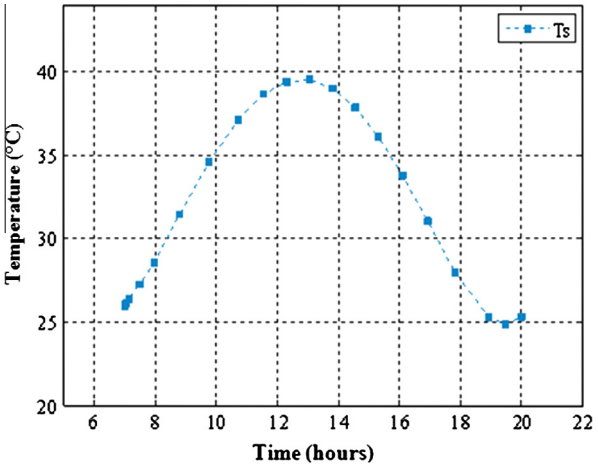

Fig. 6. Variation of the outlet temperature of the coolant in tube and sheet hybrid collector.

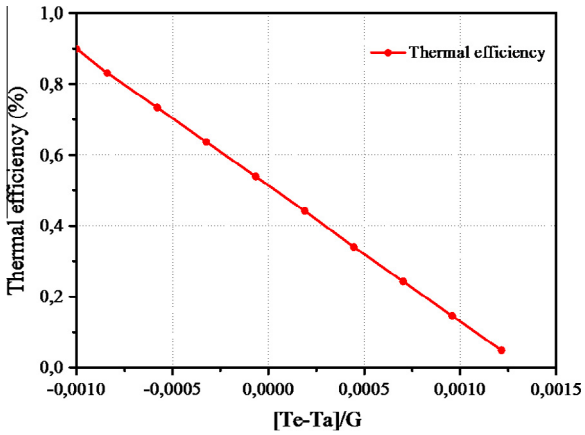

Fig. 7. Theorical Thermal efficiency of the hybrid collector.

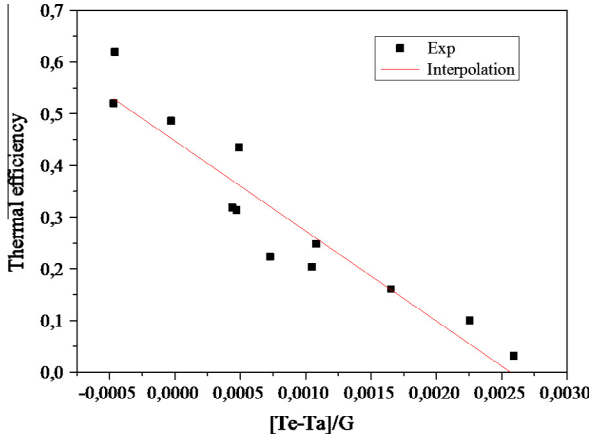

Fig. 8. Experimental Thermal efficiency of the hybrid collector with serpentine absorber.

by the inside while the outside is subject to wind action. The temperature of the coolant reaches a maximum value of 58 °C, which is an important power absorbed by the plate. Also the insulation is placed below the absorber of a high thermal conductivity, where the temperature of the inside of the insulation is important. The outlet temperature of the fluid reaches its maximum value of 40 °C between 12 AM and 2 PM.

3.2. Comparison with other configurations

There are different configurations of hybrid solar collectors that can be found in the literature. In this section we will make a comparison between the results of PVT configuration studied in this

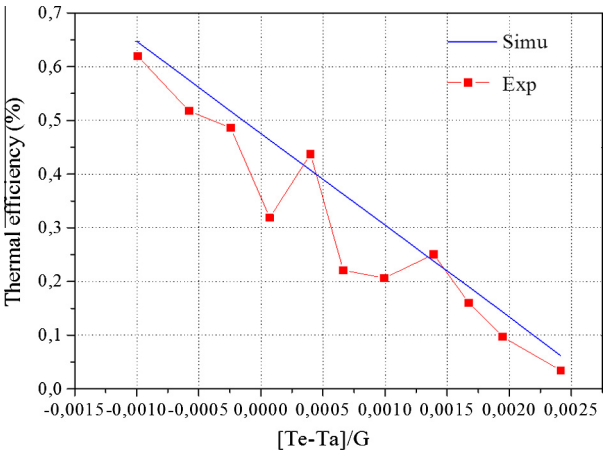

Fig. 9. Thermal efficiency of the two configurations: the thermal efficiency of serpentine with blue continued line and sheet and tube with red dot. (For interpretation of the references to color in this figure legend, the reader is referred to the web version of this article.)

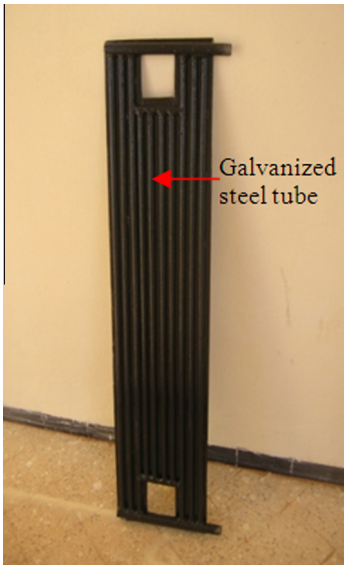

Fig. 11. Tube welded to the galvanized absorber plate.

paper which use an absorber that is composed of tube and sheet with that of reference [25], where the experimentally studied configuration is a cooper serpentine absorber.

Fig. 5 shows the temperature distribution in the hybrid collector [24], the maximum cell temperature reached was 47 °C.

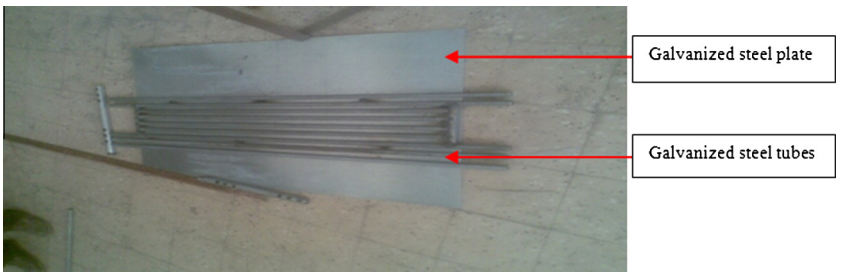

Fig. 10. Absorber plate of sheet and tube collector.

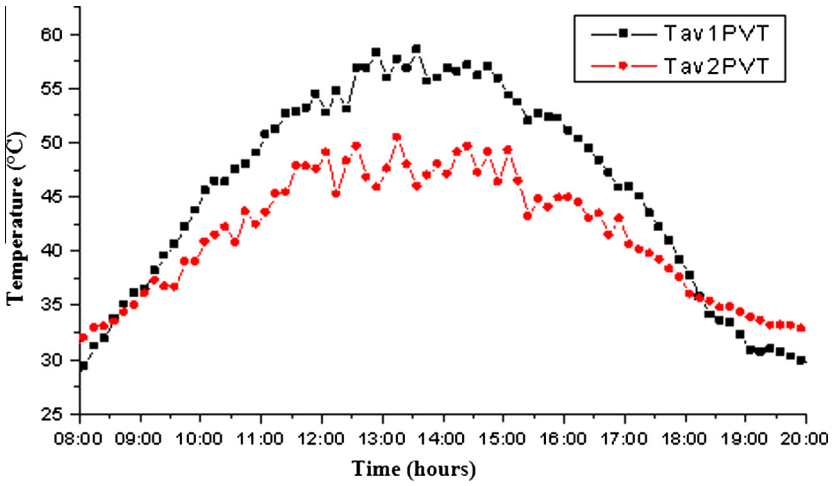

Fig. 13. Temperature of the upper and lower part of glass.

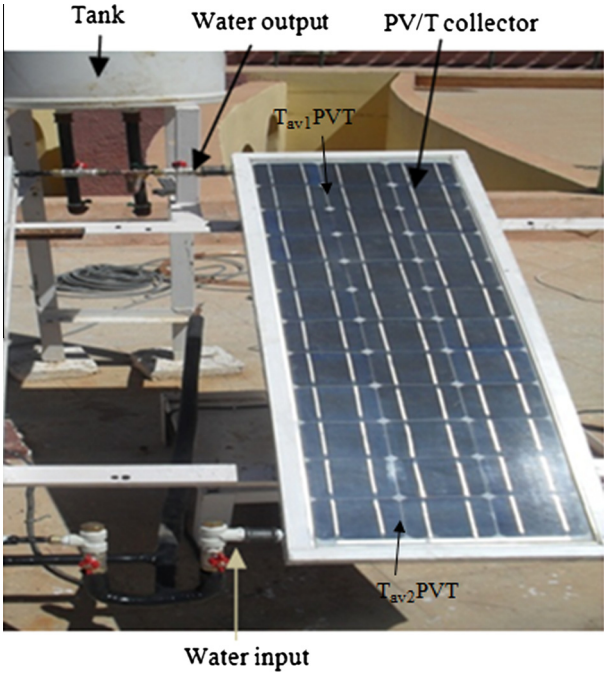

Fig. 12. Photo of the test bed.

Outlet temperatures of the coolant: From the following figures (Figs. 5 and 6), we note that outlet temperature of the fluid in the serpentine and the tube and sheet PVT reaches to 40 °C for an inlet temperature of 20 °C which shows the gain in produced thermal energy.

The thermal efficiency of the serpentine hybrid collector (Fig. 8) is lower than that of sheet and tube (which is 70% (Fig. 7).

In the aim to see better the difference between the two configurations, we put on the same figure (Fig. 9) the thermal efficiency of both configurations (serpentine with blue continued line and sheet and tube with red dot).

4. Experimental study

The heat exchanger used consists of galvanized steel tubes welded to galvanized steel plate (see Fig. 10), this interchange on the back of the photovoltaic module.

The dimensions of the tubes are: Outside diameter: 14 mm; Inner diameter: 12 mm; Spacing between the tubes: 30 mm; Diameter of 20 mm.

Fig. 11 shows the galvanized steel tubes.

Fig. 12 is a photo taken in the laboratory of the Unit for Applied Research in Renewable Energy in Ghardaïa. It shows the hybrid sheet and tubes collector placed on the control structure.

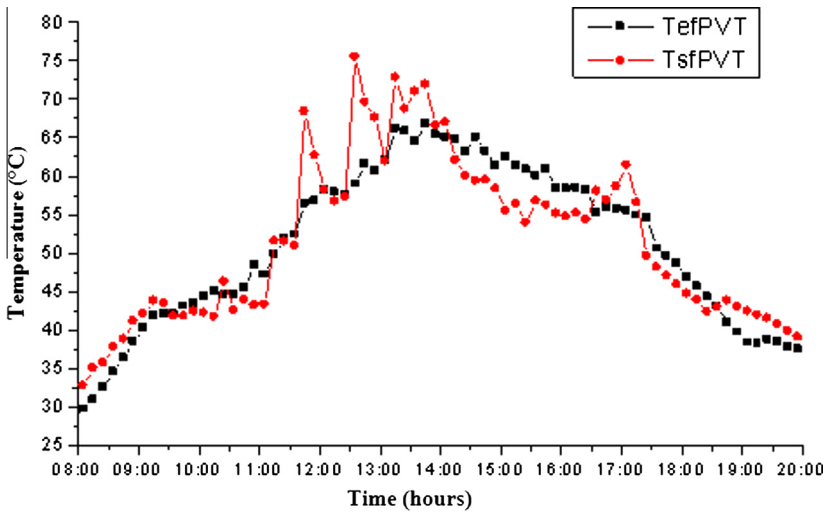

Fig. 14. Water output and input temperature of fluid.

Thermocouples type k are used to measures input and output temperature of sheet and tube PVT collector. We conducted a two mesh points in each side of the hybrid collector. Data acquisition of type 34970 (Data Acquisition/Switch Unit) is used to determine the values of temperature. The temperatures of inlet and outlet of the fluid are taken every 10 min.

The temperature at the front of the hybrid collector is shown in Fig. 13.

- T_{av1} *PVT*: Temperature of the front (on glass) the first point of the PVT collector;
- T_{av2} *PVT*: Temperature of the front (on glass) the second point of the collector;
- T_{sf} *PVT*: Output temperature of the fluid;
- T_{ef} *PVT:* Input temperature of the fluid.

The Fig. 13 shows that the temperature of the front at the top is greater than the latter at the bottom; this is due to the thermosiphon effect.

The following Fig. 14 shows the variation of temperature between the output and the input water in hybrid collector. The two curves are almost the same, except at the period from 12 am to 2 pm; the output temperature is higher than the input because the volume of water through the tubes receives satisfactory heat in this period.

5. Conclusion

There are several configurations for solar hybrid collectors, they can be classified according to the shape of the absorber used as follows: PVT with simple absorber, serpentine PVT and sheet and tube PVT absorber. The work presented in this paper concerns the theoretical and experimental study of a hybrid photovoltaic thermal solar collector or PVT. New configuration of the absorber is used. This configuration is tube and sheet galvanized steel. Our interest has studied the distribution of temperature in the different layers of the hybrid collector and we have established by numerical simulation the thermal behavior of the PVT collector. The results highlight the influence of external and internal parameters on the operating characteristics of the particular solar hybrid power generation, thermal and electrical efficiency, and overall effectiveness of the collector.

The solar radiation that is the most influencing parameter to these characteristics, and that the latter is at the same pace as the temporal variation of solar irradiance. This work allowed us to study in detail the hybrid collector with tube and sheet, determining its thermal and electrical performance. The results suggest that the PVT is a good alternative to conventional hybrid collectors.

References

[1] Zondag H. A Flat-plate, PV-thermal collectors and systems: a review. Renew Sustain Energy Rev 2005.
[2] Zondag HA, Bakker M, Helden WGJ, editors. PV/T Roadmap-a European guide for the development and market introduction of PV-thermal technology, Rapport EU-Project PV-Catapult; 2005. p. 87.
[3] Wolf M. Performance analyses of combined heating and photovoltaic power systems for residences. Energy Convers 1976;16(1–2):79–90.
[4] Hendrie SD. Photovoltaic/thermal collector development program. Rapport final. Etats-Unis: Massachusetts Institute of Technology; 1982.
[5] Raghuraman P. Analytical predictions of liquid and air photovoltaic/thermal, flat-platz collector performance. J Solar Energy Eng 1981;103(2):291–8.
[6] Cox CH, Raghuraman P. Design considerations for flat-plate-photovoltaic/thermal collectors. Solar Energy 1985;35(3):227–41.
[7] Lalovic B, Kiss Z, Weakliem HA. Hybrid amorphous silicon photovoltaic and thermal solar collector. Solar Cells 1986;19(2):131–8.
[8] Tripanagnostopoulos Y, Tzavellas D, Hybrid PV/T systems with dual heat extraction operation. In: Proceedings of the 17th European PV solar energy conference, 2001, Munich, Allemagne. p. 2515–8.
[9] Fujisawa T, Tani T. Annual exergy evaluation on photovoltaic-thermal hybrid collector. Solar Energy Mater Solar Cells 1997;47(1–4):135–48.
[10] Chow TT. Performance analysis of photovoltaic-thermal collector by explicit dynamic model. Solar Energy 2003;75:143–52.
[11] Bergene T, Lovvik OM. Model calculations on a flat-plate solar heat collector with integrated solar cells. Solar Energy 1995;55(6):453–62.
[12] Chow TT, HE W, JI J. Performance evaluation of photovoltaic-thermosyphon system for subtropical climate application. Solar Energy 2007;81:123–30.
[13] Chow TT, He W, Ji J. Hybrid photovoltaic-thermosyphon water heating system for residential application. Solar Energy 2006;80(3):298–306.
[14] Kumar S, Tiwari A. Design, fabrication and performance of a hybrid photovoltaic/thermal (PV/T) active solar still. Energy Convers Manage 2010;51:1219–29.
[15] Li M, Li G, Ji X, Yin F, Xu L. The performance analysis of the trough concentrating solar photovoltaic/thermal system. Energy Convers Manage 2011;52:2378–83.
[16] Gang P, Huide F, Jie J, Tin-tai C, Tao Z. Annual analysis of heat pipe PV/T systems for domestic hot water and electricity production. Energy Convers Manage 2012;56:8–21.
[17] Calise F, Dentice d'Accadia M, Vanoli L. Design and dynamic simulation of a novel solar trigeneration system based on hybrid photovoltaic/thermal collectors (PVT). Energy Convers Manage 2012;60:214–25.
[18] Rajoria CS, Agrawal Sanjay, Tiwari GN. Exergetic and enviro economic analysis of novel hybrid PVT array. Solar Energy 2013;88:110–9.
[19] Ammar MB, Chaabene M, Chtourou Z. Artificial neural network based control for PV/T panel to track optimum thermal and electrical power. Energy Convers Manage 2013;65:372–80.
[20] Othman Mohd Yusof, Ibrahim Adnan, Jin Goh Li, Ruslan Mohd Hafidz, Sopian Kamaruzzaman. Photovoltaic-thermal (PV/T) technology – the future energy technology. Renew Energy 2013;49:171–4.
[21] Kandilli C. Energy, performance analysis of a novel concentrating photovoltaic combined system. Energy Convers Manage 2013;67:186–96.
[22] Touafek K, Haddadi M, Malek A. Modeling and experimental validation of a new hybrid photovoltaic thermal collector. IEEE Tran Energy Convers March 2011;26(1):176–83.
[23] Touafek K, Haddadi M, Malek A. Conception and study of a low cost hybrid solar collector. In: 2nd International conference on nuclear and renewable energy resources, Ankara Turkey, 4–7 July; 2010.
[24] Touafek K, Haddadi M. Simulation numérique du comportement thermique du capteur hybride solaire photovoltaïque thermique. Rev Energies Renouvelables 2008;11(1):153–65.
[25] Touafek K, Malek A, Haddadi M, Touafek W. Electric and thermal performances of photovoltaic thermal collector in Algeria, world renewable energy congress IX and exhibition, Florence – Italy, 19–25 August 2006.